

SOLVING THE POISSON EQUATION ON A SURFACE BY REDUCTION TO A 1-DIMENSIONAL PROBLEM

CHARLES L. EPSTEIN*

Depts. of Mathematics and Radiology
University of Pennsylvania
209 South 33rd Street
Philadelphia, PA 19104

LESLIE GREENGARD†

Courant Institute
New York University
251 Mercer Street
New York, NY 10012

(Communicated by Toka Diagana)

Abstract

We describe a method for solving the Poisson equation on a surface in \mathbb{R}^3 , which, via the introduction of conformal coordinates, reduces the problem to that of solving a system of Fredholm equations of second kind on a union of smooth curves in the plane.

AMS Subject Classification: 35J05, 35Q15, 45B05, 30F10.

Keywords: Laplace equation, integral equations of the second kind, conformal coordinates, surface in Euclidean space, Riemann-Hilbert problem.

Introduction

Let Γ be a smooth closed surface in \mathbb{R}^3 with induced Riemannian metric g . In this note we explain how to find and use conformal coordinate charts to reduce the problem of solving the Poisson equation on Γ ,

$$\Delta_g u = f, \tag{0.1}$$

*E-mail address: cle@math.upenn.edu Research partially supported by NSF grant DMS06-03973 and NIH grants R21 HL088182 and R01AR053156

†E-mail address: greengard@cims.nyu.edu Research partially supported by the U.S. Department of Energy under contract DEFG0288ER25053 and by the AFOSR under MURI grant FA9550-06-1-0337

to that of solving computationally simpler problems on domains in the plane.

If the genus, p , of Γ is at least two then we reduce to solving a 2×2 -system of Fredholm equations of second kind on a union of $p + 1$ smoothly embedded simple closed curves in the plane. If the genus is 0, then we can either solve a system of Fredholm equations on a single embedded simple closed curve, or work directly on the unit sphere and use the spherical harmonic representation. Finally, if the genus is 1, then we can either solve a system of Fredholm equations on two embedded simple closed curves, or use the Fourier series representation.

1 A Riemann-Hilbert Problem for Harmonic Functions

We begin by considering a Riemann-Hilbert problem on an abstract, closed compact manifold.

Proposition 1.1. *Suppose that (M, g) is a connected, compact Riemannian manifold that can be written as a union of two components $M = M_+ \cup M_-$, which meet along a common boundary, S . Suppose that $f \in C^\infty(M)$ and on M_\pm we can find $u_\pm \in C^1(\overline{M}_\pm)$, which satisfy*

$$\Delta_g u_\pm = f \upharpoonright_{M_\pm}. \quad (1.1)$$

If

$$u_+ \upharpoonright_S = u_- \upharpoonright_S \text{ and } \frac{\partial u_+}{\partial \mathbf{v}} \upharpoonright_S = \frac{\partial u_-}{\partial \mathbf{v}} \upharpoonright_S, \quad (1.2)$$

with \mathbf{v} the outward unit normal along (relative to M_+) S , then

$$u(x) = \begin{cases} u_+(x) & \text{for } x \in M_+ \\ u_-(x) & \text{for } x \in M_- \end{cases} \quad (1.3)$$

is a smooth solution to (0.1) on M .

Proof. A simple integration by parts argument, employing (1.1) and (1.2), shows that $\Delta_g u = f$ on M in the sense of distributions. The conclusion then follows from elliptic regularity. \square

Assume that we can find \tilde{u}_\pm satisfying (1.1), with

$$\begin{aligned} [\tilde{u}_+(x) - \tilde{u}_-(x)] \upharpoonright_S &= h(x) \\ \left[\frac{\partial \tilde{u}_+}{\partial \mathbf{v}}(x) - \frac{\partial \tilde{u}_-}{\partial \mathbf{v}}(x) \right] \upharpoonright_S &= k(x); \end{aligned} \quad (1.4)$$

and functions v_\pm in $C^1(\overline{M}_\pm) \cap C^2(M_\pm)$, which satisfy

$$\begin{aligned} \Delta_g v_\pm &= 0 \text{ in } M_\pm \\ [v_+(x) - v_-(x)] \upharpoonright_S &= h(x) \\ \left[\frac{\partial v_+}{\partial \mathbf{v}}(x) - \frac{\partial v_-}{\partial \mathbf{v}}(x) \right] \upharpoonright_S &= k(x). \end{aligned} \quad (1.5)$$

The functions $u_{\pm} = \tilde{u}_{\pm} - v_{\pm}$ then satisfy the hypotheses of the Proposition, and therefore glue together to define a solution to (0.1).

Suppose that v_{\pm} are harmonic functions satisfying (1.5) for given (h, k) , then the Proposition easily implies that any other solution is of the form $v_{\pm} + c$, for a $c \in \mathbb{C}$. On the other hand, an obvious necessary condition for the solvability of this problem is that

$$\int_S k(x) dS(x) = 0. \quad (1.6)$$

The scalar Laplacian on M is a self adjoint operator, with a 1-dimensional nullspace spanned by the constant functions. We let $G(x, y)$ denote Schwartz kernel of the partial inverse, and π_0 the orthogonal projection onto the constant functions. They satisfy

$$\Delta_{g,x} G(x, y) = G(x, y) \Delta_{g,y} = \delta(x - y) - \pi_0. \quad (1.7)$$

From this identity it follows that if h is a smooth function on S and k is a smooth function, of mean zero over S , then

$$v_{\pm}(x) = \int_S G(x, y) k(y) dS(y) + \int_S \partial_{\nu, y} G(x, y) h(y) dS(y) \quad (1.8)$$

is harmonic in $M \setminus S$. As G is a classical pseudodifferential operator, with a standard asymptotic expansion along the diagonal, the jump relations along S are:

$$[v_+(x) - v_-(x)]|_S = h(x) \text{ and } [\partial_{\nu} v_+(x) - \partial_{\nu} v_-(x)]|_S = k(x). \quad (1.9)$$

This completes the proof of the following theorem:

Theorem 1.2. *If $h, k \in C^{\infty}(S)$, with k of mean zero, then the Riemann-Hilbert problem in (1.5) has a solution $v_{\pm} \in C^{\infty}(\overline{M}_{\pm})$, given by (1.8). The space of solutions is 1-dimensional and consists of $\{v_{\pm} + c : c \in \mathbb{C}\}$.*

The regularity statement in this theorem follows from the well known mapping properties of the Green's kernel, which imply the Sobolev space version of the theorem:

Corollary 1.3. *For $s \in \mathbb{R}$, if $h \in H^s(S)$, $k \in H^{s-1}(S)$, with k of mean zero, then the solution of the Riemann-Hilbert problem, v_{\pm} , given in (1.5) belongs to $H^{s+\frac{1}{2}}(M_{\pm})$. The map $\Phi : (h, k) \rightarrow (v_+, v_-)$ is continuous from*

$$\Phi : H^s(S) \oplus H_m^{s-1}(S) \rightarrow H^{s+\frac{1}{2}}(M_+) \oplus H^{s+\frac{1}{2}}(M_-).$$

Here $H_m^t(S)$ are distributions $k \in H^t(S)$ such that $\langle k, 1 \rangle = 0$.

We now turn to the special case of a surface $\Gamma \hookrightarrow \mathbb{R}^3$.

2 Surfaces in \mathbb{R}^3 and Conformal Charts

Let $\Gamma \hookrightarrow \mathbb{R}^3$ be a smooth closed surface of genus p embedded in \mathbb{R}^3 and let g denote the metric induced from the embedding. We suppose that Γ can be covered by two coordinate charts U_+, U_- , which intersect in a union of $p+1$ disjoint annuli, $\{A_j : j = 0, \dots, p\}$. We also suppose that we can find *conformal* maps:

$$\phi_{\pm} : U_{\pm} \longrightarrow \tilde{D}_{\pm} \subset \mathbb{C}. \quad (2.1)$$

Let ψ_{\pm} denote the inverses of these maps and $\phi = \phi_- \circ \psi_+$, the gluing map. This is a conformal map from $\{\phi_+(A_j) \subset \mathbb{C} : j = 0, \dots, p\}$ onto $\{\phi_-(A_j) \subset \mathbb{C} : j = 0, \dots, p\}$. We use $x^{\pm} = \phi_{\pm}(x)$, to denote the local coordinates defined by these maps.

In each annulus A_j we choose a smooth simple curve S_j , which separates A_j into two annuli. The union of these curves, S , separates Γ into two connected components $\Gamma_{\pm} \subset U_{\pm}$. We let $D_{\pm} = \phi_{\pm}(\Gamma_{\pm}) \subset \tilde{D}_{\pm}$; these are smoothly bounded planar domains, diffeomorphic to a disk with p disjoint sub-disks removed. We now show how to use this conformal representation of Γ to reduce the problem of solving the Poisson equation on Γ :

$$\Delta_g u = f, \quad (2.2)$$

to that of solving a system of second kind integral equations on S .

We let Δ_0 denote the flat Euclidean Laplacian, $\partial_x^2 + \partial_y^2$, and

$$G_0(x, y) = \frac{1}{2\pi} \log |x - y|, \quad (2.3)$$

its fundamental solution in \mathbb{R}^2 . Because the maps ϕ_{\pm} are conformal, the local coordinate representations of the Laplace operator are of the form

$$\Delta_g \upharpoonright_{\tilde{D}_{\pm}} = \frac{1}{j_{\pm}^2(x^{\pm})} \Delta_0, \quad (2.4)$$

where

$$\psi_{\pm}^*(dA_g) = j_{\pm}^2(x^{\pm}) dx_1^{\pm} dx_2^{\pm}. \quad (2.5)$$

If f is a function of mean zero on Γ , then we let f also denote its pullbacks to \tilde{D}_{\pm} . The functions

$$\tilde{u}_{\pm}(x^{\pm}) = \int_{\tilde{D}_{\pm}} G_0(x^{\pm}, y^{\pm}) f(y^{\pm}) j_{\pm}^2(y^{\pm}) dy^{\pm} \quad (2.6)$$

pulled back to Γ solve

$$\Delta_g \tilde{u}_{\pm} = f \upharpoonright_{U_{\pm}}. \quad (2.7)$$

We can pull this formula back to U_{\pm} to obtain

$$\tilde{u}_{\pm}(x) = \int_{U_{\pm}} G_0(\phi_{\pm}(x), \phi_{\pm}(y)) f(y) dA_g(y). \quad (2.8)$$

If, as before, we let $G(x, y)$ denote the Schwartz kernel of the partial inverse of Δ_g , then these relations imply that on $U_\pm \times U_\pm$ we have

$$\Delta_{g,x}[G_0(\phi_\pm(x), \phi_\pm(y)) - G(x, y)] = -\frac{1}{A_\Gamma} = \Delta_{g,y}[G_0(\phi_\pm(x), \phi_\pm(y)) - G(x, y)], \quad (2.9)$$

with A_Γ the area of Γ . Therefore

$$(\Delta_{g,x} + \Delta_{g,y})[G_0(\phi_\pm(x), \phi_\pm(y)) - G(x, y)] = -\frac{2}{A_\Gamma}. \quad (2.10)$$

Elliptic regularity therefore shows

Proposition 2.1. *There are functions $m_\pm(x, y) \in C^\infty(U_\pm \times U_\pm)$ so that*

$$G_0(\phi_\pm(x), \phi_\pm(y)) - G(x, y) = m_\pm(x, y). \quad (2.11)$$

An important corollary of (2.11) is the fact that

$$G_0(\phi_+(x), \phi_+(y)) - G_0(\phi_-(x), \phi_-(y)) = m_+(x, y) - m_-(x, y). \quad (2.12)$$

Hence, we do not need to know the Schwartz kernel, $G(x, y)$, to compute the difference: $m_+(x, y) - m_-(x, y)$.

Let the jumps in \tilde{u}_\pm and $\partial_v \tilde{u}_\pm$ across S be denoted by h and k respectively. If f has mean zero over Γ , then Green's formula implies that k has mean zero over S , as required for the solvability of the Riemann-Hilbert problem. We now need to find harmonic functions \tilde{v}_\pm defined in Γ_\pm that satisfy the jump conditions:

$$[\tilde{v}_+(x) - \tilde{v}_-(x)]|_S = h(x) \text{ and } [\partial_v \tilde{v}_+(x) - \partial_v \tilde{v}_-(x)]|_S = k(x). \quad (2.13)$$

We use corrections of the form

$$\tilde{v}_\pm(x) = \int_S [G_0(\phi_\pm(x), \phi_\pm(y))a(y) + \partial_{v,y}G_0(\phi_\pm(x), \phi_\pm(y))b(y)]ds_g(y). \quad (2.14)$$

Proposition 2.1 easily gives formulæ for the jumps in v_\pm and $\partial_v v_\pm$ across S :

$$\begin{aligned} [\tilde{v}_+(x) - \tilde{v}_-(x)] &= b(x) + \int_S [m_+(x, y) - m_-(x, y)]a(y)ds_g(y) + \\ &\quad \int_S \partial_{v,y}[m_+(x, y) - m_-(x, y)]b(y)ds_g(y), \end{aligned} \quad (2.15)$$

$$\begin{aligned} \partial_v[\tilde{v}_+(x) - \tilde{v}_-(x)] &= -a(x) + \int_S \partial_{v,x}[m_+(x, y) - m_-(x, y)]a(y)ds_g(y) + \\ &\quad \int_S \partial_{v,x}\partial_{v,y}[m_+(x, y) - m_-(x, y)]b(y)ds_g(y). \end{aligned} \quad (2.16)$$

To actually solve this problem we need to pull these equations back to the plane. For this purpose we use the coordinate map ψ_+ . The difference in the fundamental solutions $m_+ - m_-$ now takes a simple explicit form:

$$n(x^+, y^+) = m_+(x^+, y^+) - m_-(x^+, y^+) = G_0(x^+, y^+) - G_0(\varphi(x^+), \varphi(y^+)). \quad (2.17)$$

The fact that φ is conformal leads immediately to the following basic result

Lemma 2.2. *For $x, y \in bD_+$ we have the relation*

$$G_0(x, y) = G_0(\varphi(x), \varphi(y)) + n(x, y), \quad (2.18)$$

where $n \in C^\infty(bD_+ \times bD_+)$.

Proof. This is a consequence of Proposition 2.1, but it is instructive to give a different proof. There is nothing to prove unless x and y are close together. In this case we see that, for $x \neq y$,

$$G_0(\varphi(x), \varphi(y)) = \frac{1}{2\pi} \log |x - y| + \frac{1}{2\pi} \log \left| \frac{\varphi(x) - \varphi(y)}{x - y} \right|. \quad (2.19)$$

Because φ is analytic in a neighborhood of bD_+ we see that the second term above can be rewritten as

$$\frac{1}{2\pi} \log \left| \frac{\varphi(x) - \varphi(y)}{x - y} \right| = \frac{1}{2\pi} \log \left| \sum_{j=1}^{\infty} \frac{\varphi^{[j]}(y)}{j!} (x - y)^{j-1} \right|. \quad (2.20)$$

As $\varphi'(y)$ does not vanish on bD_+ this completes the proof of the lemma. \square

To rewrite equations in the (x^+, y^+) variables we need to relate ds^+ , Euclidean arclength along bD_+ , to ds_g , and $\partial_{v,x}$ to ∂_{v,x^+} along S . An elementary computation, using the fact that ψ_+ is conformal, shows that we have the relations

$$\psi_+^* ds_g(x^+) = j_+(x^+) ds^+ \text{ and } \partial_{v,x} = \psi_{+*} \left[\frac{1}{j_+(x^+)} \partial_{v,x^+} \right], \quad (2.21)$$

where the conformal factor j_+ is defined in (2.5). The integral equations can now be rewritten as:

$$h(x^+) = b(x^+) + \int_{bD_+} n(x^+, y^+) a(y^+) j_+(y^+) ds^+(y^+) + \int_{bD_+} \partial_{v,y^+} n(x^+, y^+) b(y^+) ds^+(y^+), \quad (2.22)$$

$$k(x^+) = -a(x^+) + \int_{bD_+} \frac{1}{j_+(x^+)} \partial_{v,x^+} n(x^+, y^+) a(y^+) j_+(y^+) ds^+(y^+) + \int_{bD_+} \frac{1}{j_+(x^+)} \partial_{v,x^+} \partial_{v,y^+} n(x^+, y^+) b(y^+) ds^+(y^+). \quad (2.23)$$

As $n(x^+, y^+)$ is a smooth function on bD_+ Equations (2.22) and (2.23) are a system of Fredholm equations of the second kind.

The data $h(x^+)$ and $k(x^+)$ can easily be computed from the local coordinate representations of \tilde{u}_\pm :

$$\tilde{u}_\pm(x^\pm, y^\pm) = \int_{\tilde{D}_\pm} G_0(x^\pm, y^\pm) f(y^\pm) j_\pm^2(y^\pm) dy^\pm, \quad (2.24)$$

along with the relations in (2.21). If, as we have assumed, the conformal maps $\{\phi_\pm\}$ are defined in an open cover of Γ , then the boundaries of D_\pm lie in the interior of the domains of definition of \tilde{u}_\pm , which should facilitate the numerical evaluation of $h(x^+)$ and $k(x^+)$. For numerical purposes, we can also insert smooth cutoff functions into these integrals, so long as they take the value 1 on \tilde{D}_\pm .

If a pair (a, b) is in the null-space of the system of equations (2.22) and (2.23), then the harmonic functions \tilde{v}_\pm , defined in (2.14), glue together along S to define a harmonic function on all of Γ , which must therefore be constant. For such data, the pair of harmonic functions

$$v_\pm(x) = \int_{bD_\pm} [G_0(x, y) a(y) j_\pm(y) \pm \partial_{v, y} G_0(x, y) b(y)] ds^\pm(y), \quad (2.25)$$

assume the same constant value in D_\pm , respectively. The difficulty in characterizing the null-space arises because the extensions of $v_\pm(x)$ to D_\pm^c defined by the integral formula in (2.25), do *not*, in general, agree with the pull-backs of v_\mp via the gluing map ϕ . Hence, our hypothesis does not immediately imply that the functions v_\pm are constant across bD_\pm , and therefore zero. We leave the problem of characterizing the null-space of this system of equations to a subsequent publication. We consider the problem of constructing the necessary conformal maps in the following section.

3 Finding Conformal Charts

We briefly describe how to find conformal coordinate charts on a surface, Γ , embedded in \mathbb{R}^3 . Finding such coordinates usually entails solving the Laplace equation on the surface, or at least on subdomains of the surface, and is therefore only worth the effort if one needs to repeatedly solve the inhomogeneous equation:

$$\Delta_\Gamma u = f. \quad (3.1)$$

We describe an approach to this problem, which works in all cases. It assumes that Γ is covered by two *smooth* coordinate charts, of planar character, which are then “corrected” to give conformal coordinate charts.

For the most part we are considering surfaces with genus $p \geq 2$. If the genus is either 0 or 1, then the Riemann-Hilbert approach described above can be used, but it is also possible to use a more global approach. If the genus is 0, then a conformal mapping, $\phi : \Gamma \rightarrow S_1^2$, can be constructed. Here S_1^2 is the unit sphere in \mathbb{R}^3 . This case is discussed in considerable detail in the monograph [2]. Equation (3.1) can then be replaced with

$$\frac{1}{\rho^2} \Delta_{S_1^2} u = f, \quad (3.2)$$

where $\phi^*(\rho^2 ds_{S_1^2}^2) = g$, the metric induced on Γ by its embedding into \mathbb{R}^3 . The equation can be solved using, e.g., spherical harmonics. The torus case, $p = 1$, is considered in Section 4.

For Γ of genus p , we assume that it is divided into two smoothly bounded regions Γ_{\pm} of planar character, which meet along a union of $p + 1$ simple closed curves. We can find two open subsets U_{\pm} as described above, which intersect in a union of $p + 1$ disjoint annular regions $\{A_j : j = 0, \dots, p\}$, so that $b\Gamma_{\pm}$ is a relatively compact subset of the union of these annuli. It is usually very difficult to find conformal maps from multiply connected regions onto “model domains,” e.g. domains bounded by circles. On the other hand, for the method described above to work, it is only necessary that we map U_{\pm} conformally onto smoothly bounded regions of the plane, with no necessity to carefully control the geometry of the boundary of the image.

Starting with the cover of Γ by two open sets $U_{\pm} \supset \Gamma_{\pm}$, of planar character, we suppose that there are smooth one-to-one maps

$$\widehat{\Psi}_{\pm} : \widehat{D}_{\pm} \longrightarrow U_{\pm}, \quad (3.3)$$

with \widehat{D}_{\pm} smoothly bounded domains in \mathbb{R}^2 . In other words the open subsets U_{\pm} are represented parametrically over bounded domains in the plane. Topologically, the domains \widehat{D}_{\pm} are disks with p holes removed. We suppose, without loss of generality, that the bD_{\pm} is a union of $p + 1$ smooth, simple closed curves, which we denote $\{C_j^{\pm} : j = 0, 1, \dots, p\}$. Here C_0^{\pm} bound the unbounded components of the complements of \widehat{D}_{\pm} , and, for $1 \leq j \leq p$,

$$C_j^{\pm} = bB_j^{\pm}, \quad (3.4)$$

where the $\{B_j^{\pm}\}$ are topological disks.

The pullback by $\widehat{\Psi}_{\pm}$ of the induced metric on Γ is represented by a smooth family of symmetric, positive definite 2×2 -matrices.

$$\widehat{\Psi}_{\pm}^*(g) = \sum_{1 \leq i, j \leq 2} g_{ij}^{\pm} dx_i dx_j. \quad (3.5)$$

To find a conformal representation, we extend the metric tensor smoothly into the bounded components of the complement, $B^{\pm} = \cup_{j=1}^p B_j^{\pm}$. Let $\widetilde{D}_{\pm} = \widehat{D}_{\pm} \cup B^{\pm}$. The space of symmetric, positive definite matrices is a convex cone, and therefore we only need to extend g_{ij}^{\pm} to a small neighborhood of bB^{\pm} . Using a partition of unity we can then interpolate from these extensions to the identity matrix. We also use g_{ij}^{\pm} to denote the extended metric tensor. Using this approach, the conformal structure on a large part of B^{\pm} can be made to agree with the standard structure on \mathbb{C} .

The simply connected domains \widetilde{D}_{\pm} have globally defined metrics. Therefore we can use the Laplace operator defined by this metric to find conformal maps onto the unit disk, $\widetilde{\Phi}_{\pm} : \widetilde{D}_{\pm} \rightarrow \mathbb{D}_1$, which carry C_0^{\pm} onto $b\mathbb{D}_1$. A standard method would be to find real harmonic functions, u_{\pm} , on \widetilde{D}_{\pm} with an interior logarithmic singularity, vanishing on the boundary of \widetilde{D}_{\pm} . For simplicity, we can place the logarithmic singularity in the interior of B^{\pm} , where the conformal structure defined by the metric agrees with the standard one. The harmonic conjugates v_{\pm} are easily found by integration, and then

$$\widetilde{\Phi}_{\pm} = e^{u_{\pm} + iv_{\pm}} \quad (3.6)$$

defines a conformal map of \tilde{D}_\pm onto the unit disk. This method is described in [3]. If we let D_\pm denote the image of \tilde{D}_\pm under the maps $\tilde{\phi}_\pm$, and $\tilde{\psi}_\pm$ the inverses of $\tilde{\phi}_\pm$, then the compositions

$$\Psi_\pm = \hat{\psi}_\pm \circ \tilde{\psi}_\pm : D_\pm \longrightarrow U_\pm \quad (3.7)$$

are conformal maps.

Once these conformal maps are found, we can use the method described in Section 2 to solve the Poisson equation on Γ . Of course, to find the conformal coordinates we need to solve the Poisson equation on domains in Γ . Once these coordinates are found, the problem of solving the Poisson equation is reduced to that of applying the Newtonian potential to functions on the coordinate charts, and the solution of a second kind integral equation on a union of smooth curves. The application of the Newtonian potential can be accelerated using a fast multi-pole method, (see [1]) and the integral equation is on a one-dimensional set rather than a two-dimensional set. Once the work of finding the conformal maps is done, these two steps can presumably be done much faster than the direct solution of the Poisson equations by a non-sparse, 2-dimensional method. As noted above, this method will prove efficacious when the Poisson equation has to be solved repeatedly for a variety of right hand sides, on a fixed embedded surface. The accuracy of the overall method will be determined by the accuracy of the computation of the conformal maps, Ψ_\pm .

4 The Torus Case

The torus, $p = 1$, is a special case in that if $\Gamma \subset \mathbb{R}^3$ is a surface of genus 1, then we can choose two embedded circles a_1, b_1 so that $\Gamma \setminus a_1 \cup b_1$ is homeomorphic to a disk. Moreover there is a conformal map

$$\phi : \Gamma \setminus a_1 \cup b_1 \longrightarrow R, \quad (4.1)$$

where R is a region in \mathbb{C} bounded by a parallelogram. If ω is a real harmonic 1-form on Γ then $dz = \omega + i\star_2\omega$ is a holomorphic $(1,0)$ -form; here \star_2 is the Hodge star-operator defined by the metric on Γ . Integrating this form then defines the map ϕ . Using this coordinate representation we can reduce the problem of solving the Laplace equation on Γ to that of solving the Euclidean Laplace equation on R , with periodic boundary conditions. This can easily be done using a Fourier representation. In this case, as in the case of genus 0, the Riemann-Hilbert step is not needed, as the Fourier representation automatically imposes the needed periodic boundary conditions.

If Γ is a torus of revolution, then the conformal coordinate can be found quite explicitly. Under this hypothesis, there are periodic functions $(r(t), z(t))$ defined on \mathbb{R} so that Γ is the image of the map

$$(t, s) \rightarrow (r(t) \cos s, r(t) \sin s, z(t)). \quad (4.2)$$

In these coordinates the metric on the surface takes the form

$$g = r^2(t)ds^2 + [(r'(t))^2 + (z'(t))^2]dt^2. \quad (4.3)$$

Without loss of generality we can assume that the generator is parameterized by arclength, that is:

$$(r'(t))^2 + (z'(t))^2 = 1. \quad (4.4)$$

The area form is then given by

$$dA = r(t)ds \wedge dt. \quad (4.5)$$

A simple calculation shows that

$$\omega = ds \quad (4.6)$$

is a harmonic form with

$$\star_2 \omega = \frac{dt}{r(t)}. \quad (4.7)$$

We introduce the new parameter

$$b(t) = \int_0^t \frac{d\tau}{r(\tau)}. \quad (4.8)$$

If we let $t(b)$, denote the inverse of $t \rightarrow b(t)$, then the map

$$(b, s) \rightarrow (r(t(b)) \cos s, r(t(b)) \sin s, z(t(b))) \quad (4.9)$$

is a conformal map from a rectangle $R \subset \mathbb{C}$ to $\Gamma \subset \mathbb{R}^3$. Suppose the rectangle is $R = [0, S] \times [0, B]$; the Laplace equation on Γ takes the form

$$\frac{1}{\rho(b)^2} [\partial_s^2 + \partial_b^2] u = f(s, b), \quad (4.10)$$

where ρ is B -periodic and both u and f are S -periodic in s and B -periodic in b . As usual this equation is solvable if and only if $\rho^2(b)f(s, b)$ has mean 0. In this case,

$$\rho(b)^2 f(s, b) = \sum_{(m,n) \neq (0,0)} f_{mn} e^{\frac{2\pi i m s}{S}} e^{\frac{2\pi i n b}{B}}, \quad (4.11)$$

and

$$u(s, b) = -\frac{S^2 B^2}{4\pi^2} \sum_{(m,n) \neq (0,0)} \frac{f_{mn} e^{\frac{2\pi i m s}{S}} e^{\frac{2\pi i n b}{B}}}{m^2 B^2 + n^2 S^2}. \quad (4.12)$$

The Fourier representation of $\rho^2 f$ and the solution of the Laplace equation can both be accomplished with spectral accuracy by sampling f on a uniformly spaced grid (in the (s, b) -coordinates) and using the standard discrete Fourier transform to approximate the Fourier integrals and inverse Fourier transform.

5 Numerical Examples

We close this paper by considering the special case of a circular torus, so that the generator of Γ is a round circle. We can parameterize Γ on the rectangle $-\pi \leq t < \pi$ and $0 \leq s < 2\pi$ by setting:

$$(r(t), z(t)) = (R + r \cos t, r \sin t), \quad (5.1)$$

with $r < R$. This is not a conformal representation. The metric induced by the embedding into \mathbb{R}^3 is given by

$$g = (R + r \cos t)^2 \left(ds^2 + \frac{r^2}{(R + r \cos t)^2} dt^2 \right). \quad (5.2)$$

This parameterization of the generator has constant speed, equal to r , which is adequate for our purposes. In this case

$$\star_2 \omega = db = \frac{rdt}{R + r \cos t}, \quad (5.3)$$

integrating we find that

$$b = \mu \tan^{-1} \left[\lambda \tan \left(\frac{t(b)}{2} \right) \right], \text{ where } \mu = \frac{2r}{\sqrt{R^2 - r^2}} \text{ and } \lambda = \sqrt{\frac{R-r}{R+r}}. \quad (5.4)$$

Solving we obtain that

$$t(b) = 2 \tan^{-1} \left[\frac{1}{\lambda} \tan \left(\frac{b}{\mu} \right) \right]. \quad (5.5)$$

The natural parameter domain is the rectangle:

$$R = \{(s, b) : 0 \leq s < 2\pi, -\mu \frac{\pi}{2} \leq b < \mu \frac{\pi}{2}\}. \quad (5.6)$$

In the (b, s) coordinates the metric induced on the embedded torus takes the form

$$g = \rho^2(b)(ds^2 + db^2), \quad (5.7)$$

where

$$\rho(b) = \frac{R-r}{\sin^2(b/\mu) + \lambda^2 \cos^2(b/\mu)}. \quad (5.8)$$

Because the map from the (s, b) -plane to the embedded torus is conformal, the coefficient ρ measures the metric distortion between the induced metric on the embedded torus and the flat metric $ds^2 + db^2$. A simple calculation shows that this distortion varies between $R+r$ and $R-r$, and therefore λ^2 gives a measure of the variability of the mesh size in the image domain, produced as the image of a uniform rectangular grid in the (s, b) -plane. Observe that, in the ambient coordinates of \mathbb{R}^3 we have

$$e^{is} = \frac{x+iy}{\sqrt{x^2+y^2}} \text{ and } \cos \left(\frac{2b}{\mu} \right) = \frac{R\sqrt{x^2+y^2} + r^2 - R^2}{r\sqrt{x^2+y^2}}. \quad (5.9)$$

Our first plots show the distortions which result from different choices of (r, R) . In Figure 1(a) we show the mesh obtained with 32×32 -grid with $r = 1$ and $R = 1.2$. In Figure 1(b) we show the mesh obtained with 32×32 -grid with $r = 2$ and $R = 16$. As predicted there is considerable variation in the size of the image grid in the first case where $\lambda^2 = 1/11$, as compared to the second case, where $\lambda^2 = 7/9$.

To test the accuracy of our algorithm, we begin with

$$\begin{aligned} f_n &= \operatorname{Re} \left[\frac{(x+iy)^n}{(x^2+y^2)^{\frac{n+2}{2}}} \right] \\ g_n &= \operatorname{Re} \left[\frac{(x+iy)^n}{(x^2+y^2)^{\frac{n+2}{2}}} \right] \left[\frac{R\sqrt{x^2+y^2}+r^2-R^2}{r\sqrt{x^2+y^2}} \right]. \end{aligned} \quad (5.10)$$

The formulae in (5.9) show that

$$\rho^2(b)f_n(b,s) = \sin ns \text{ and } \rho^2(b)g_n(b,s) = \sin ns \cos\left(\frac{2b}{\mu}\right), \quad (5.11)$$

and therefore the solutions to $\Delta_g u_n = f_n$ and $\Delta_g v_n = g_n$ are

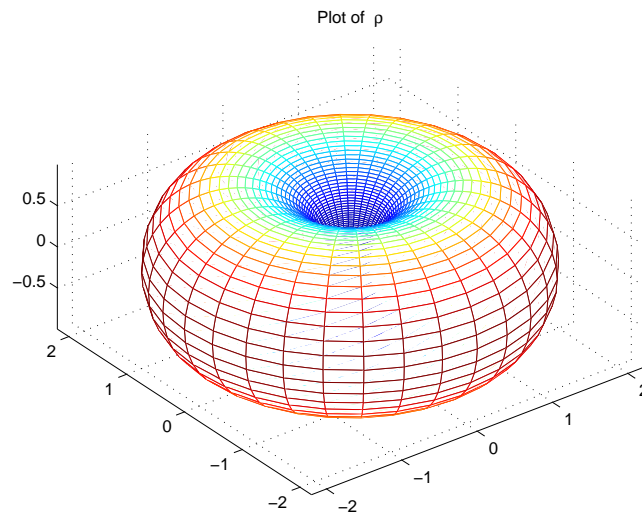
$$u_n = \frac{-1}{n^2} \sin ns \text{ and } v_n = \frac{-1}{n^2 + \left(\frac{2b}{\mu}\right)^2} \sin ns \cos\left(\frac{2b}{\mu}\right). \quad (5.12)$$

Our numerical experiments show that as soon as the number of samples in the s -direction exceeds the Nyquist rate, the error in the numerical solution essentially equals the machine accuracy (about 10^{-16}). We show several pairs (f_4, u_4) , (f_{32}, u_{32}) , and (g_{16}, v_{16}) . in Figure 2. In these examples we take $r = 1$ and $R = 2$.

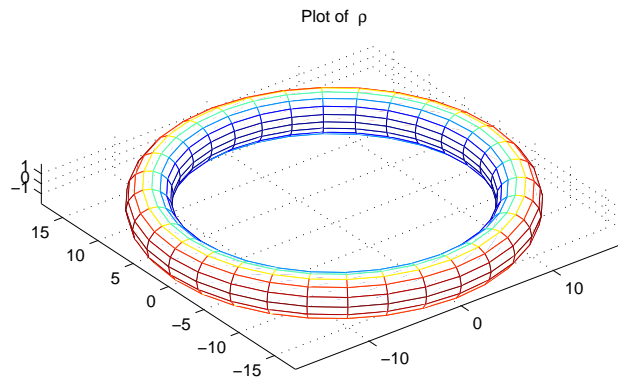
We conclude with a pair of examples involving more complicated right hand sides. In Figure 3 we show the solution with $f = \cos x \cos 3y \sin 5z$, and in Figure 4, the solution with $f = \exp(-((x+3)^2 + y^2 + z^2)) - c$. (Here c is selected so that f has mean zero.) For these examples $r = 1$ and $R = 2$, moreover we use 256 points in the s direction and 512 points in the b -direction.

References

- [1] L. Greengard, The Rapid Evaluation of Potential Fields in Particle Systems, MIT Press, Cambridge, MA, 1988.
- [2] X. D. Gu and S.-T. Yau, Computational Conformal Geometry, vol. 3 of Advanced Lectures in Mathematics, International Press, Somerville, MA, 2008.
- [3] Z. Nehari, Conformal Mapping, Dover Publications, Inc., New York, NY, 1952.



(a) 32×32 grid with $r = 1, R = 1.2$.



(b) 32×32 grid with $r = 2, R = 16$.

Figure 1. Examples showing the distortion in the image grid.

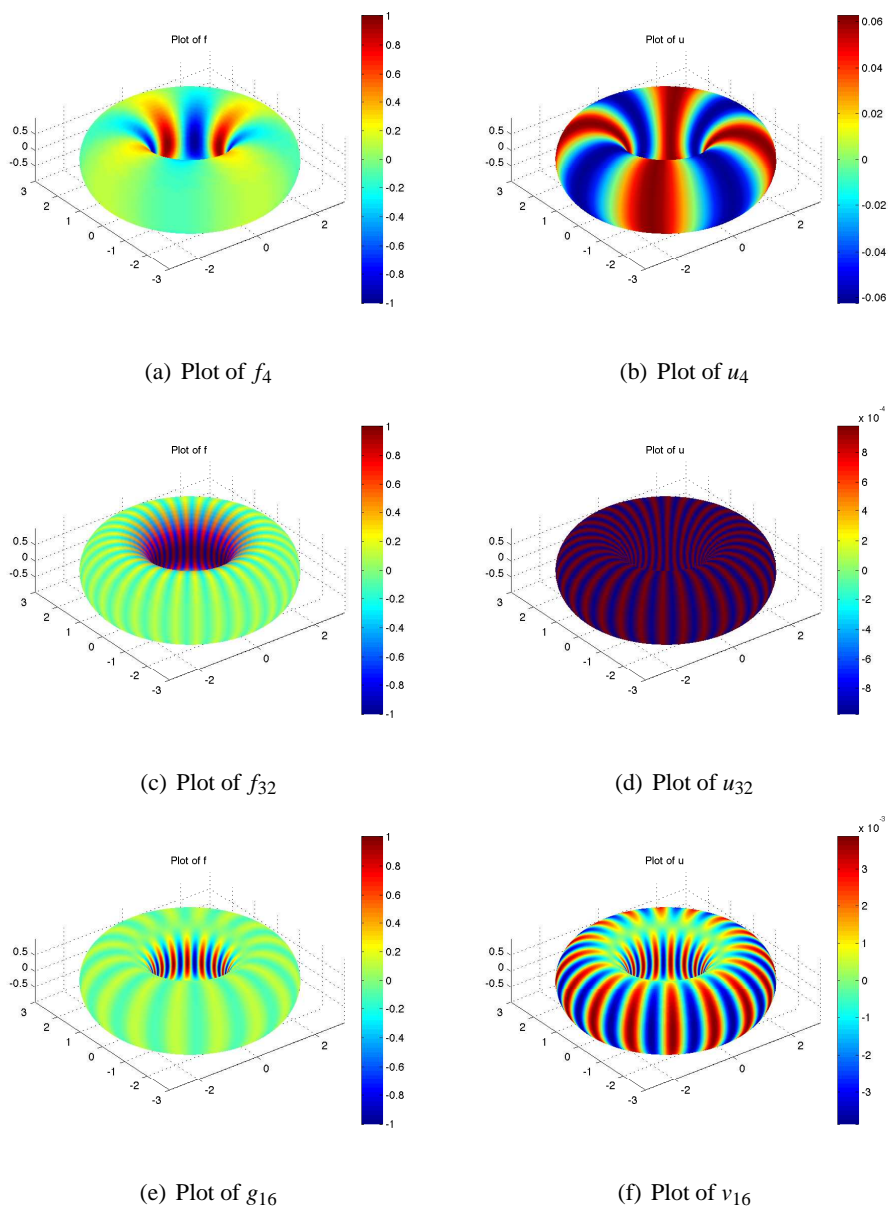


Figure 2. Examples where the exact solution is known.

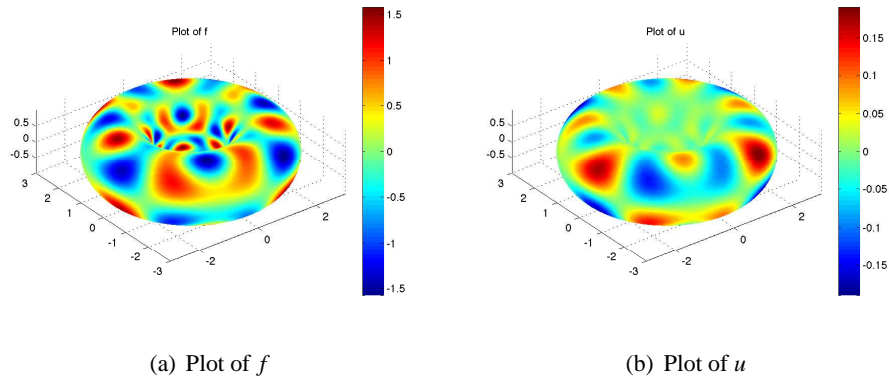


Figure 3. $f = \cos x \cos 3y \sin z$

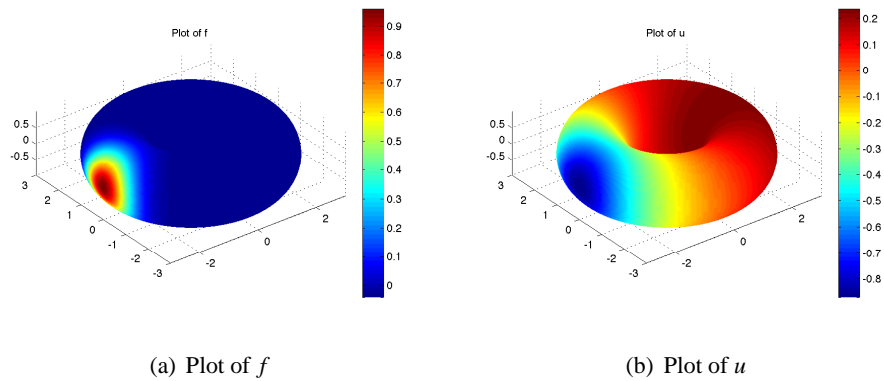


Figure 4. $f = \exp(-((x+3)^2 + y^2 + z^2)) - c$